

Reducing gravity takes the bounce out of running

Delyle T. Polet,^{1,‡} Ryan T. Schroeder,² John E. A. Bertram³

Keywords: bipedal running, reduced gravity, leg swing, energetics, optimization, biomechanics

Summary Statement: During running, humans take higher leaps in normal gravity than in reduced gravity, in order to optimally balance the competing costs of stance and leg-swing work.

Abstract

In gravity below Earth normal, a person should be able to take higher leaps in running. We asked ten subjects to run on a treadmill in five levels of simulated reduced gravity and optically tracked center of mass kinematics. Subjects consistently *reduced* ballistic height compared to running in normal gravity. We explain this trend by considering the vertical takeoff velocity (defined as maximum vertical velocity). Energetically optimal gaits should balance energetic costs of ground-contact collisions (favouring lower takeoff velocity), and step frequency penalties such as leg swing work (favouring higher takeoff velocity, but less so in reduced gravity). Measured vertical takeoff velocity scaled with the square root of gravitational acceleration, following energetic optimality predictions and explaining why ballistic height decreases in lower gravity. The success of work-based costs in predicting this behaviour challenges the notion that gait adaptation in reduced gravity results from an unloading of the stance phase. Only the relationship between takeoff velocity and swing cost changes in reduced gravity; the energetic cost of the down-to-up transition for a given vertical takeoff velocity does not change with gravity. Because lower gravity allows an elongated swing phase for a given takeoff velocity, the motor control system can relax the vertical momentum change in the stance phase, so reducing ballistic height, without great energetic penalty to leg swing work. While it may seem counterintuitive, using less “bouncy” gaits in reduced gravity is a strategy to reduce energetic costs, to which humans seem extremely sensitive.

Introduction

Under normal circumstances, why do humans and animals select particular steady gaits from the myriad possibilities available? One theory is that the chosen gaits minimize metabolic energy expenditure (Alexander and Jayes, 1983; Ruina et al., 2005). To test this theory, one can subject organisms to abnormal circumstances. If the gait changes to a new energetic optimum, it can be inferred that energetics also govern gait choice under normal conditions (Bertram and Ruina, 2001; Long and Srinivasan, 2013; Selinger et al., 2015).

¹Department of Biological Sciences, University of Calgary, Calgary T2N 1N4, Canada ²Biomedical Engineering, University of Calgary, Calgary T2N 1N4, Canada ³Cumming School of Medicine, University of Calgary, Calgary T2N 1N4, Canada [‡]Author for correspondence: dtpolet@ucalgary.ca

28 One “normal” gait is the bipedal run, and one abnormal circumstance is that of reduced gravity. Movie
29 1 demonstrates the profound effect reducing gravity has on running kinematics. A representative subject
30 runs at 2 m s^{-1} in both Earth-normal and simulated lunar gravity (about one-sixth of Earth-normal). The
31 change in kinematics is apparent; the gait in normal gravity involves pronounced center-of-mass undulations
32 compared to the near-flat trajectory of the low-gravity gait. While center-of-mass vertical excursions during
33 stance are known to decrease in reduced gravity (Donelan and Kram, 2000), we observed that the height
34 achieved in the flight phase also decreases. This gait modification seems paradoxical: in reduced gravity,
35 people are free to run with much higher leaps. Instead, they seem to flatten their gait. Why should this be?

36 A simple explanation posits that the behaviour is energetically beneficial. To explore the energetic
37 consequences of choosing to run with lower leaps in reduced gravity, we first considered the impulsive model
38 of running, following Rashevsky (1948) and Bekker (1962), which treats a human runner as a point mass
39 body bouncing off rigid vertical limbs (Fig. 1). Stance is treated as an inelastic, impulsive collision with
40 the ground. In reality, stance occurs in finite time, and elastic mechanisms exist. However, the inelastic
41 approximation is remarkably productive in explaining gait choice (Ruina et al., 2005). When we use the
42 term “energetic cost of collisions”, we are generally referring to non-recoverable energy loss during stance
43 resulting from some interaction of the center of mass with the ground (Bertram and Hasaneini, 2013). Such
44 losses may arise from damping, active negative work or discontinuous velocity profiles. In any case, modelling
45 these interactions as an inelastic collision provides a simple estimation of the net cost.

46 During this collision, all vertical velocity is lost while horizontal velocity is conserved (Fig. 1b). The
47 total kinetic energy lost per step is therefore $E_{\text{col}} = mV^2/2$, where m is the runner’s mass and V is their
48 vertical takeoff velocity¹. Lost energy must be recovered through muscular work to maintain a periodic gait,
49 and so an energetically-optimal gait will minimize these losses. If center-of-mass kinetic energy loss were the
50 only source of energetic cost, then the optimal solution would always be to minimize vertical takeoff velocity.
51 However, such a scenario would require an infinite stepping frequency as V approaches zero (Alexander,
52 1992; Ruina et al., 2005), as step frequency (ignoring stance time and air resistance) is $f = g/(2V)$, where
53 g is gravitational acceleration.

54 Let us suppose there is an energetic penalty that scales with step frequency, as $E_{\text{freq}} \propto f^k \propto g^k/V^k$,
55 where $k > 0$. Such a penalty may arise from work-based costs associated with swinging the leg, which
56 are frequency-dependent ($k = 2$; Alexander, 1992; Doke et al., 2005), or from short muscle burst durations
57 recruiting less efficient, fast-twitch muscle fibres ($k \approx 3$; Kram and Taylor, 1990; Kuo, 2001). Notably, this
58 penalty increases with gravity, since the non-contact duration will be shorter for any given takeoff velocity
59 in higher gravity. The penalty also has minimal cost when V is maximal; smaller takeoff velocities require
60 more frequent steps, which is costly. Therefore, the two sources of cost act in opposite directions: collisional
61 loss promotes lower takeoff velocities, while frequency-based cost promotes higher takeoff velocities.

62 If these two effects are additive, then it follows that the total cost per step is

$$\begin{aligned} E_{\text{tot}} &= E_{\text{col}} + E_{\text{freq}} \\ &= mV^2/2 + Ag^k/V^k \end{aligned} \quad (1)$$

66 where A is an unknown proportionality constant relating frequency to energetic cost. As the function is
67 continuous and smooth for $V > 0$, a minimum can only occur either at the boundaries of the domain, or

¹ In this paper, we are taking the vertical takeoff velocity as the maximum vertical velocity during the gait cycle, following Cavagna (2006). However, this is not always equal to the vertical velocity at toe-off, and this distinction complicates the analysis. These complications are addressed in the discussion.

68 when $\frac{\partial E_{\text{tot}}}{\partial V} = 0$. Solving the latter equation for V yields

$$69 \quad V^* \propto g^{k/(k+2)} \quad (2)$$

70 as the unique critical value. Here the asterisk denotes a predicted (optimal) value. Since E_{tot} approaches
71 infinity as V approaches 0 and infinity (Eqn 1), the critical value must be the global minimum in the domain
72 $V > 0$. As $k > 0$, it follows from Eqn 2 that the energetically-optimal solution is to reduce the vertical
73 takeoff velocity as gravity decreases.

74 The observation² of He et al. (1991) that $V \propto \sqrt{g}$ implies $k = 2$, a finding consistent with frequency costs
75 arising from the work of swinging the limb (Alexander, 1992; Doke et al., 2005). However, their empirical
76 assessment of the relationship used a small sample size, with only four subjects. We tested the prediction of
77 Eqn 2 by measuring the maximum vertical velocity over each running stride, as a proxy for takeoff velocity,
78 in ten subjects using a harness that simulates reduced gravity. We also measured the maximum vertical
79 displacement in the ballistic phase to verify whether the counter-intuitive observation of lowered ballistic
80 center-of-mass height in hypogravity, as exemplified in Movie 1, is a consistent feature of reduced gravity
81 running.

82 **Materials and Methods**

83 We asked ten healthy subjects to run on a treadmill for two minutes at 2 m s^{-1} in five different gravity levels
84 (0.15, 0.25, 0.35, 0.50 and 1.00 G, where G is 9.8 m s^{-2}). A belt speed of 2 m s^{-1} was chosen as a comfortable,
85 intermediate jogging pace that could be accomplished at all gravity levels. Reduced gravities were simulated
86 using a harness-pulley system similar to that used by Donelan and Kram (2000), but differing in the use of a
87 spring-pendulum system to generate near-constant force for a large range of motion. Hasaneini et al. (2017
88 preprint) provide more details of the apparatus. The University of Calgary Research Ethics Board approved
89 the study protocol and informed consent was obtained from all subjects. Leg length for each subject was
90 measured during standing from the base of the shoe to the greater trochanter on one leg.

91 Due to the unusual experience of running in reduced gravity, subjects were allowed to acclimate at their
92 leisure before indicating they were ready to begin each two-minute measurement trial. In each case, the
93 subject was asked to simply run in any way that felt comfortable. Data from 30 to 90 s from trial start
94 were analyzed, providing a buffer between acclimating to experimental conditions at trial start and initiating
95 slowdown at trial end.

96 **Implementation and measurement of reduced gravity**

97 Gravity levels were chosen to span a broad range. Of particular interest were low gravities, at which the
98 model predicts unusual body trajectories. Thus, low levels of gravity were sampled more thoroughly than
99 others. The order in which gravity levels were tested was randomized for each subject, so as to minimize
100 sequence conditioning effects.

101 For each gravity condition, the simulated gravity system was adjusted in order to modulate the force
102 pulling upward on the subject. In this particular harness, variations in spring force caused by support spring
103 stretch during cyclic loading over the stride were virtually eliminated using an intervening lever (see Figs 3
104 and 4 in Hasaneini et al., 2017, preprint). The lever moment arm was adjusted in order to set the upward

² In reality, He et al. (1991) measured vertical speed at initial foot contact, but for the impulsive model in its simplest form, this is indistinguishable from takeoff velocity.

105 force applied to the harness, and was calibrated with a known set of weights prior to all data collection.
106 A linear interpolation of the calibration was used to determine the moment arm necessary to achieve the
107 desired upward force, given subject weight and targeted effective gravity. Using this system, the standard
108 deviation of the upward force during a trial (averaged across all trials) was 3% of the subject's Earth-normal
109 body weight.

110 Achieving exact target gravity levels was not possible since the lever's moment arm is limited by discrete
111 force increments (approximately 15 N). Thus, each subject received a slight variation of the targeted gravity
112 conditions, depending on their weight. A real-time data acquisition system allowed us to measure tension
113 forces at the gravity harness and calculate the effective gravity level at the beginning of each new condition.
114 The force-sensing system consisted of an analog strain gauge (Micro-Measurements CEA-06-125UW-350),
115 mounted to a C-shaped steel hook connecting the tensioned cable and harness. The strain gauge signal
116 was passed to a strain conditioning amplifier (National Instruments SCXI-1000 amp with SCXI-1520 8-
117 channel universal strain gauge module connected with SCXI-1314 terminal block), digitized (NI-USB-6251
118 mass termination) and acquired in a custom virtual instrument in LabView. The tension transducer was
119 calibrated with a known set of weights once before and once after each data collection trial to correct
120 for modest drift error in the signal. The calibration used was the mean of the pre- and post-experiment
121 calibrations.

122 Center of mass kinematic measurements

123 A marker was placed at the lumbar region of the subject's back, approximating the position of the center
124 of mass. Each trial was filmed at 120 Hz using a Casio EX-ZR700 digital camera. The marker position was
125 digitized in DLTdv5 (Hedrick, 2008). Position data were differentiated using a central differencing scheme
126 to generate velocity profiles, which were further processed with a 4th-order low-pass Butterworth filter at 7
127 Hz cutoff. The vertical takeoff velocity was defined as the maximum vertical velocity during each gait cycle
128 (V in Fig. 1). This definition corresponds to the moment at the end of stance where the net vertical force
129 on the body is null, in accordance with a definition of takeoff proposed by Cavagna (2006).

130 Vertical takeoff velocities were identified as local maxima in the vertical velocity profile. Filtering and
131 differentiation errors occasionally resulted in some erroneous maxima being identified. To rectify this, first
132 any maxima within ten time steps of data boundaries were rejected. Second, the stride period was measured
133 as time between adjacent maxima. If any stride period was 25% lower than the median stride period or less,
134 the maxima corresponding to that stride period were compared and the largest maximum kept, with the
135 other being rejected. This process was repeated until no outliers remained.

136 Position data used to determine ballistic height were processed with a 4th-order low-pass Butterworth
137 filter at 9 Hz cutoff. Ballistic height was defined as the vertical displacement from takeoff to the maximum
138 height within each stride. No outlier rejection was used to eliminate vertical position data peaks, since the
139 filtering was slight and no differentiation was required. If a takeoff could not be identified prior to the point
140 of maximum height within half the median stride time, the associated measurement of ballistic height was
141 rejected; this strategy prevented peaks from being associated with takeoff from a different stride.

142 Statistical methods

143 Takeoff velocities and ballistic heights were averaged across all gait cycles in each trial for each subject. To
144 test whether ballistic height varied with gravity, a linear model between ballistic height and gravitational

145 acceleration was fitted to the data using least squares regression, and the validity of the fit was assessed
146 using an F -test. A linear model was also tested for $\log(V)$ against $\log(g)$ using the same methods. Since
147 the proportionality coefficient between V^* and \sqrt{g} is unknown *a priori*, we derived its value from a least
148 squares best fit of measured vertical takeoff velocity against the square root of gravitational acceleration,
149 setting the intercept to zero. Given a minimal correlation coefficient of 0.5 and sample size of 50, a *post-hoc*
150 power analysis yields statistical power of 0.96, with type I error margin of 0.05. Data were analyzed using
151 custom scripts written in MATLAB (v. 2016b).

152 Results

153 Response of Ballistic Height and Takeoff Velocity to Gravity

154 Data from all trials are shown in Fig. 2. Ballistic height increases with gravity (Fig. 2A, linear vs constant
155 model, $p = 4 \times 10^{-4}$, $R^2 = 0.24$, $N = 50$), validating the counter-intuitive result exemplified in Movie 1 as
156 a consistent feature of running in hypogravity.

157 Takeoff velocity also increases with gravitational acceleration (Fig. 2B), and a least-squares fit of Eqn 2
158 using $k = 2$ follows empirical measurements well ($R^2 = 0.73$, $N = 50$). Other values of k were also tested (Fig
159 3). If the impulsive model is accurate, then the best-fit slope of a scatter plot of $\log(V)$ against $\log(g)$ should
160 correspond to $k/(k + 2)$ (Eqn 2), that is, slopes of 0.33, 0.50 or 0.60 for $k = 1, 2$ and 3 respectively. Only
161 the slope predicted by $k = 2$ falls within the 95% confidence interval of the least squares slope (0.47 ± 0.09 ;
162 Fig. 3).

163 A best fit at $k = 2$ implies a frequency-based cost arising primarily from the work of leg swing. However,
164 since only the center of mass is offloaded by the harness, the natural frequency of limb swing remains
165 unchanged for all target gravity levels (Donelan and Kram, 2000). Since metabolic energy of swing is
166 minimal at natural frequency (Doke et al., 2005), it is necessary to adjust the predictions from the impulsive
167 model (Appendix A). An adjusted model exhibits a fit with $R^2 = 0.745$ ($N = 50$, Fig. A1), only marginally
168 better than the simple model with $k = 2$ ($R^2 = 0.73$, Fig. 2B). The predictions do not change greatly,
169 because time spent in the air *is* affected by gravity, and more air time requires less work to swing the legs,
170 regardless of natural frequency³.

171 Predicting Ballistic Height Trends

172 The impulsive model with $k = 2$ predicts that the ballistic height should remain constant (dash line in Fig.
173 2A). This constant value agrees with empirical data at low g , but exhibits increasing error towards normal
174 g .

175 We defined “takeoff” as occurring when the net force on the body was null and velocity was maximal;
176 however, this does not equate to the moment when the stance foot leaves the ground. After the point
177 of maximal velocity, upward ground reaction forces decay to zero. During this time, the net downward
178 acceleration on the body is less than gravitational acceleration. Thus, the body travels higher than would
179 be expected if maximal velocity corresponded exactly to the point where the body entered a true ballistic
180 phase, as in the model (Fig. 1).

181 We can account for the missing impulse with the spring-mass model. This model describes the kinematics
182 and dynamics of running well (McMahon and Cheng, 1990; He et al., 1991; Blickhan and Full, 1993), and

³ As long as stride frequency is greater than natural frequency, which is very likely the case for the present study (Appendix A)

183 provides a way to estimate stance time from takeoff velocity (though it lacks the ability to *predict* takeoff
184 velocity; McMahon and Cheng, 1990). Notably, correcting the prediction $V \propto \sqrt{g}$ with spring-mass model
estimates of finite stance yields the following relationship for ballistic height (Appendix B):

$$185 \quad H = \frac{g}{2\omega_0^2} + \frac{A^2}{2}, \quad (3)$$

186 where ω_0 is the natural angular frequency of vertical oscillation, and A is a constant in the relationship
187 $V = A\sqrt{g}$. Note that Eqn 3 is linear in g , and approaches the predictions from the impulsive model alone
188 as $g \rightarrow 0$. Taking $\omega_0 \approx 18 \text{ rad s}^{-1}$ from He et al. (1991), and A from the best-fit in Fig. 2B, Eqn 3 gives
189 the dot-dash line shown in Fig. 2A. The predicted relationship (Eqn 3) has a slope of 0.015 m G^{-1} and an
190 intercept of 0.03 m , and is within the 95% confidence interval of the best-fit slope ($0.021 \pm 0.01 \text{ m G}^{-1}$) and
191 intercept ($0.029 \pm 0.006 \text{ m}$), indicating that finite stance accounts for the discrepancy within error, though
192 it underpredicts the true slope somewhat.

193 Discussion

194 Human runners lower the height achieved in the ballistic phase as gravity decreases. This adaptation requires
195 pronounced modification of the takeoff velocity, since maintaining the latter parameter in all conditions would
196 result in substantially increased ballistic height in reduced gravity. Why human runners would modify their
197 gait so greatly was initially unclear.

198 A simple work-based model of energetic cost explains the trends well. The fit in Fig. 2B exhibits an
199 R^2 value of 0.73, indicating that a simple energetic model can explain over two thirds of the variation in
200 maximum vertical velocity resulting from changes in gravity. Human runners seem to be sensitive to these
201 energetic costs and adjust their takeoff velocity accordingly. However, the model has its limitations, and an
202 accounting of finite stance (which was initially neglected in the model) was necessary to explain the trend of
203 increasing ballistic height with gravity. Despite the updated model matching the general trend of the data,
204 the slope in Eqn 3 is reduced compared to the empirically-derived slope.

205 The use of the external lumbar point as a center of mass approximation may explain some of the remaining
206 difference between Eqn 3 and observation. At lower gravity, the body maintained a relatively erect, rigid
207 posture (as exemplified by Movie 1), and so the lumbar marker likely follows the center of mass closely.
208 However, at higher gravity, the legs move through larger excursions and the torso exhibits slight rotation,
209 making the lumbar estimate less accurate. At normal gravity, Slawinski et al. (2004) showed that the lumbar
210 point overestimates vertical oscillations of the flight phase (by less than 1 cm)– though their trials were at a
211 high belt speed (5 m s^{-1}). If the same results hold in our case, we would expect that the measured ballistic
212 height in Fig. 2A should be slightly lower at higher levels of gravity, reducing the actual slope and possibly
213 improving the agreement to Eqn 3. Future work could use a multisegment model to improve center of mass
214 and ballistic height measurements, but such a technique is unlikely to reverse the trend of increasing ballistic
215 height with gravitational acceleration.

216 The present results indicate that the cost of step frequency is a key factor in locomotion. Although the
217 exact value of the optimal takeoff velocity depends on both frequency-based penalties and collisional costs,
218 the former penalties change with gravity while the latter do not (Fig. 4). The collisional cost landscape
219 is independent of gravity because the final vertical landing velocity is alone responsible for the lost energy.
220 Regardless of gravitational acceleration, vertical landing speed must equal vertical takeoff speed in the model;

221 so a particular takeoff velocity will have a particular, unchanging collisional cost.

222 However, taking off at a particular vertical velocity results in greater flight time at lower levels of gravity;
223 thus, the frequency-based cost curves are decreased as gravity decreases (Fig. 4). Frequency-based costs,
224 particularly limb-swing work, appear to be an important determinant of the effective movement strategies
225 available to the motor control system. Their apparent influence warrants further investigation into the extent
226 of their contribution to metabolic expenditure.

227 While the present study corroborates others in finding that a work-based cost ($k = 2$) predicts locomotion
228 well (Alexander, 1980, 1992; Hasaneini et al., 2013), other authors have favoured a higher-order “force/time”
229 cost (Kuo, 2001; Doke et al., 2005; Doke and Kuo, 2007). Interestingly, a higher-order model in frequency
230 cost ($k = 3$) did not fit the present data; however, our simple model with $k = 3$ only approximates the
231 force/time cost in the swing phase, and does not account for a rate cost during stance. Further research
232 must be done to distinguish the predictive value of work-based cost to its alternatives; however, for the
233 present results, a work-based model is sufficient, at least for takeoff velocity.

234 The present results challenge the notion that metabolic cost of running is determined largely by the cost
235 of generating force during stance (Kram and Taylor, 1990; Arellano and Kram, 2014), purportedly supported
236 by the observation that metabolic cost is proportional to gravity (Farley and McMahon, 1992). According
237 to the best-fit model presented here, the net cost (Eqn 1) at optimal takeoff velocity (Eqn 2) is expected to
238 increase in proportion to gravitational acceleration (that is, $E_{\text{tot}}(V^*) \propto g$), as Farley and McMahon observed
239 (1992). The cost of vertical acceleration of the center of mass can decrease as gravity is reduced *only* because
240 the relationship between takeoff velocity and swing cost changes; this allows the subject to settle on a lower
241 stance cost, whose relationship to takeoff velocity does *not* change as a function of gravity (Fig. 4). These
242 trends can be explained simply from muscular work, and do not rely on any independent force-magnitude
243 cost.

244 The model presented in this article is admittedly simple and makes unrealistic assumptions, including
245 impulsive stance, no horizontal muscular force, non-distributed mass, and a simple relationship between
246 step frequency and energetic cost. Further, horizontal accelerations will incur a larger portion of energetic
247 losses as horizontal speed increases (Willems et al., 1995), and the tradeoff between swing and stance costs
248 may change. The present model would not be able to anticipate any such trend, as it has no dependence
249 on horizontal speed. Future investigations could evaluate work-based costs using more advanced optimal
250 control models (Srinivasan and Ruina, 2006; Hasaneini et al., 2013), eliminating some of these assumptions
251 and allowing for an investigation into horizontal speed dependence. Despite its simplicity, the impulsive
252 model with work-based swing cost is able to correctly predict the observed trends in takeoff velocity with
253 gravity, and demonstrates that understanding the energetic cost of both swing and stance is critical to
254 evaluating why the central nervous system selects specific running motions in different circumstances.

255 Although many running conditions are quite familiar, running in reduced gravity is outside our general
256 experience. Surprisingly, releasing an individual from the downward force of gravity does not result in higher
257 leaps between foot contacts. Rather, humans use less bouncy gaits with slow takeoff velocities in reduced
258 gravity, taking advantage of a reduced collisional cost while balancing a stride-frequency penalty.

259 List of Symbols

| | |
|------------|--|
| θ | leg angle (radians) |
| ω_0 | vertical natural angular frequency in the spring-mass model (radians s^{-1}) |

| | |
|--------------------|--|
| A | proportionality constant in the relationship $E_{\text{freq}} = Af^k$ (J s ^k) |
| B | proportionality constant in the relationship $E_{\text{swing}} = Bml^2(f^2 - f_n^2)$ |
| E_{col} | energetic cost of collisions (J) |
| E_{freq} | energetic cost related to step-frequency (J) |
| E_{swing} | energetic cost of leg swing work (J) |
| E_{tot} | total energetic cost ($E_{\text{col}} + E_{\text{freq}}$ or $E_{\text{col}} + E_{\text{swing}}$, in J) |
| f | step frequency (Hz) |
| f_n | natural pendular frequency (Hz) |
| g | gravitational acceleration (m s ⁻²) |
| G | Earth-normal gravitational acceleration (9.8 m s ⁻²) |
| Gr | Groucho number ($\equiv v\omega_0/g$) |
| H | ballistic height (m) |
| I | leg moment of inertia about the hip (kg m ²) |
| k | exponent in proportionality $E_{\text{freq}} \propto f^k$ |
| l | leg length (m) |
| m | total subject mass (kg) |
| r | length change from leg rest length (m) |
| t | time after toe-down (s) |
| t^* | time at which maximum vertical speed is achieved (s) |
| t_m | time at which maximum vertical velocity is achieved (s) |
| t_s | stance period (s) |
| U | average horizontal speed (m s ⁻¹) |
| v | vertical velocity at toe-off (m s ⁻¹) |
| V | vertical velocity at takeoff (maximum vertical velocity, in m s ⁻¹) |
| V^* | optimal and predicted vertical takeoff velocity (m s ⁻¹) |

260 Acknowledgements

261 The authors would like to thank Art Kuo, Jim Usherwood, David Lee and Allison Smith for comments on
262 earlier drafts, as well as two anonymous reviewers who provided constructive insights that greatly improved
263 the manuscript.

264

265 Competing Interests

266 The authors declare no competing financial interests.

267

268 Author Contributions

269 All authors assisted in designing the experiment, collecting data and writing the manuscript; D.T.P. conceived
270 the energetics-based model and performed data analysis. All authors gave final approval for submission.

271

272 Funding

273 This work was funded by the Natural Sciences and Engineering Research Council of Canada [CGSD3-459978-
274 2014 to D.T.P., 312117-2012 to J.E.A.B.]

275

276 Data Availability

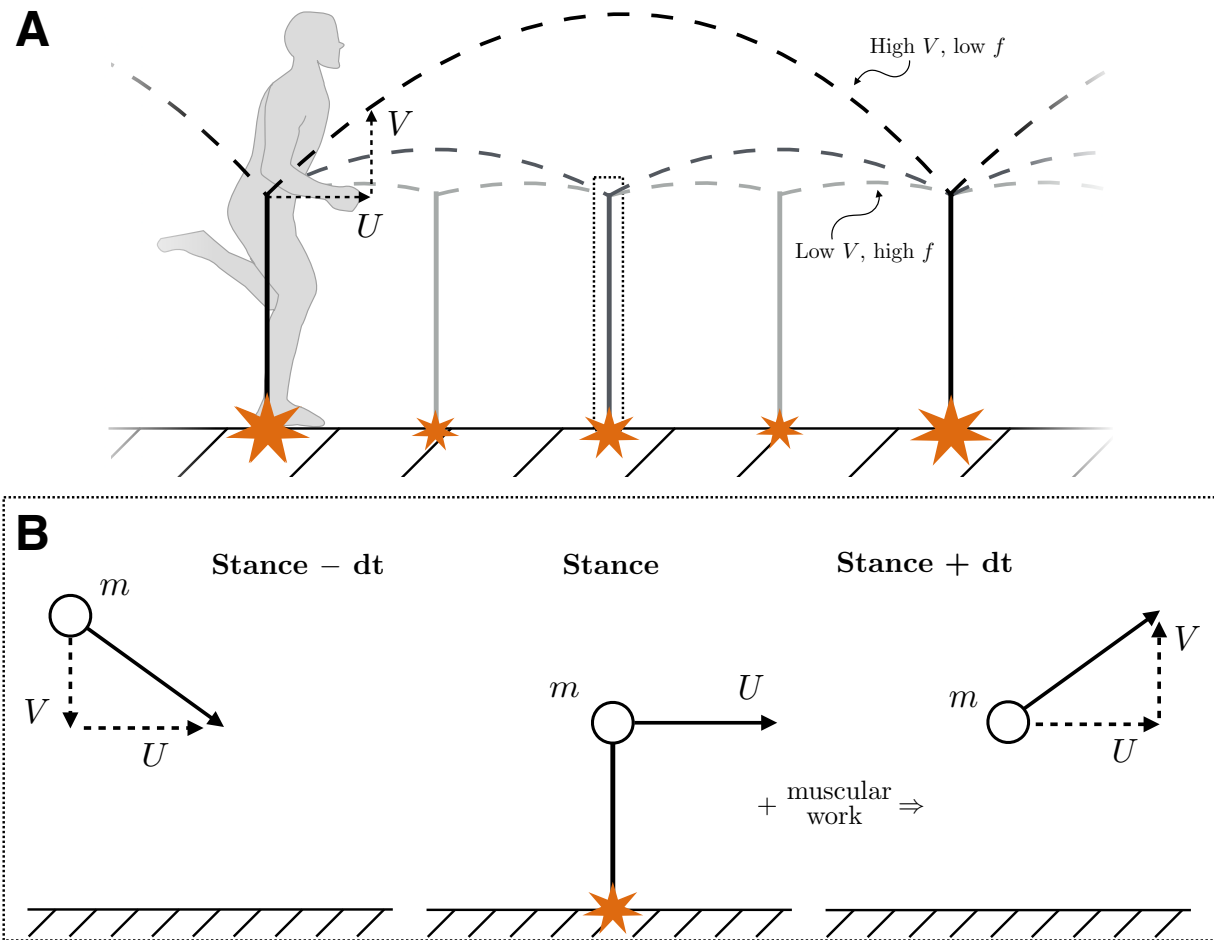
277 The dataset supporting this article has been uploaded as part of the supplementary material (Table S1).

278 References

- 279 **Alexander, R. M.** (1980). Optimum walking techniques for quadrupeds and bipeds. *J. Zool.* **192**, 97–117.
- 280 **Alexander, R. M.** (1992). A Model of Bipedal Locomotion on Compliant Legs. *Philos. Trans. R. Soc.*
281 *Lond. B Biol. Sci.* **338**, 189–198.
- 282 **Alexander, R. M. and Jayes, A. S.** (1983). A dynamic similarity hypothesis for the gaits of quadrupedal
283 mammals. *J. Zool.* **201**, 135–152.
- 284 **Arellano, C. J. and Kram, R.** (2014). Partitioning the metabolic cost of human running: A task-by-task
285 approach. *Integr. Comp. Biol.* **54**, 1084–1098.
- 286 **Bekker, M. G.** (1962). II. Locomotion in nature. In *Theory of Land Locomotion*, pp. 4–26. Ann Arbor,
287 MI: University of Michigan Press, 2 edition.
- 288 **Bertram, J. E. A. and Hasaneini, S. J.** (2013). Neglected losses and key costs: Tracking the energetics
289 of walking and running. *J. Exp. Biol.* **216**, 933–938.
- 290 **Bertram, J. E. A. and Ruina, A.** (2001). Multiple walking speed–frequency relations are predicted by
291 constrained optimization. *J. Theor. Biol.* **209**, 445–453.
- 292 **Blickhan, R. and Full, R.** (1993). Similarity in multilegged locomotion: Bouncing like a monopode. *J.*
293 *Comp. Physiol. A.* **173**, 509–517.
- 294 **Cavagna, G. A.** (2006). The landing-take-off asymmetry in human running. *J. Exp. Biol.* **209**, 4051–4060.
- 295 **Doke, J., Donelan, J. M. and Kuo, A. D.** (2005). Mechanics and energetics of swinging the human leg.
296 *J. Exp. Biol.* **208**, 439–445.
- 297 **Doke, J. and Kuo, A. D.** (2007). Energetic cost of producing cyclic muscle force, rather than work, to
298 swing the human leg. *J. Exp. Biol.* **210**, 2390–2398.
- 299 **Donelan, J. M. and Kram, R.** (2000). Exploring dynamic similarity in human running using simulated
300 reduced gravity. *J. Exp. Biol.* **203**, 2405–2415.
- 301 **Farley, C. T. and Ferris, D. P.** (1998). Biomechanics of walking and running: Center of mass movements
302 to muscle action. *Exerc. Sport Sci. Rev.* **26**, 253–286.
- 303 **Farley, C. T. and McMahon, T. A.** (1992). Energetics of walking and running: Insights from simulated
304 reduced-gravity experiments. *J. Appl. Physiol.* **73**, 2709–2712.
- 305 **Hasaneini, S. J., Macnab, C., Bertram, J. E. A. and Leung, H.** (2013). The dynamic optimization
306 approach to locomotion dynamics: Human-like gaits from a minimally-constrained biped model. *Adv.*
307 *Robot.* **27**, 845–859.
- 308 **Hasaneini, S. J., Schroeder, R. T., Bertram, J. E. A. and Ruina, A.** (2017). The converse effects
309 of speed and gravity on the energetics of walking and running. *bioRxiv* doi:10.1101/201319.

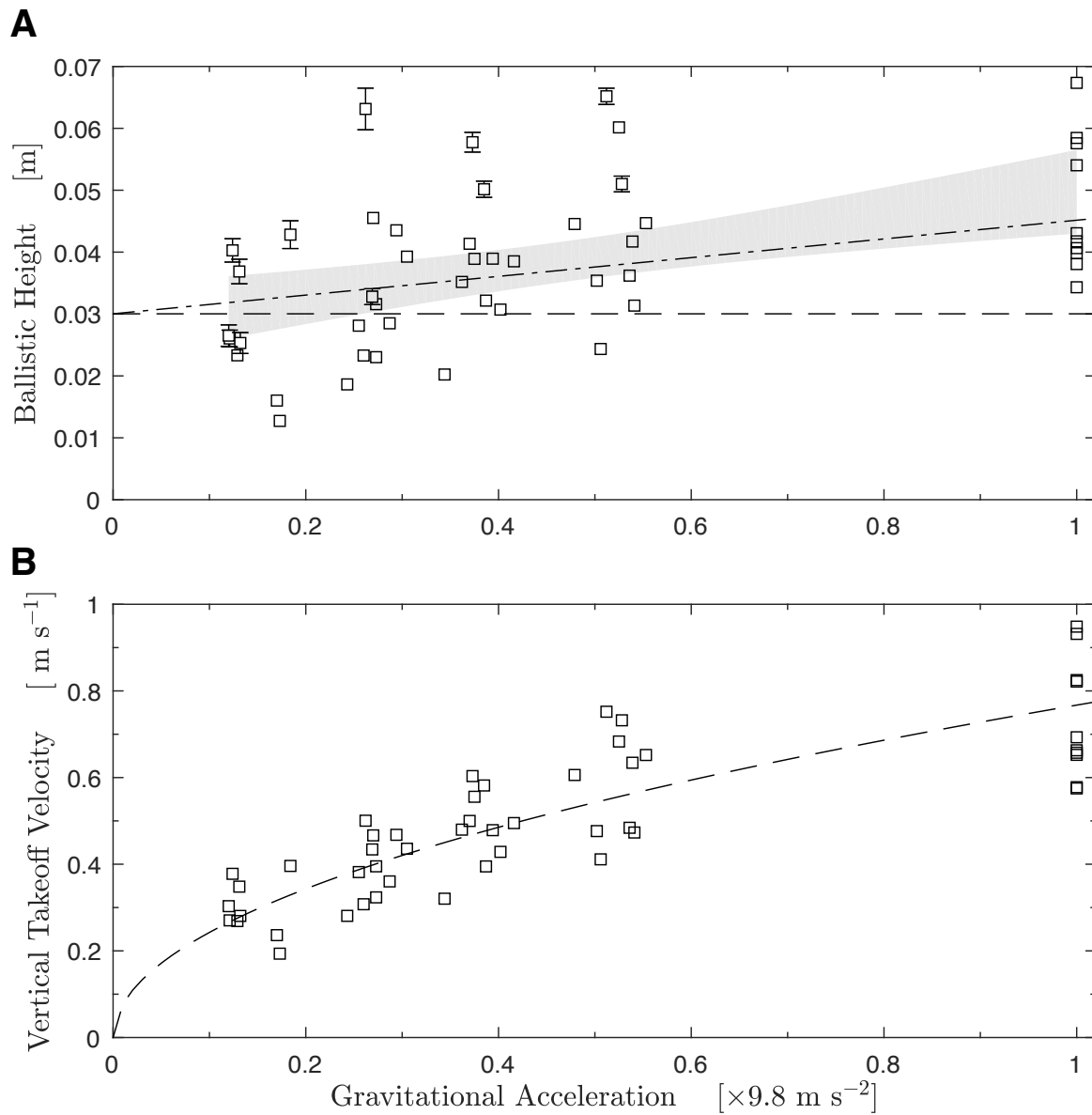
- 310 **He, J. P., Kram, R. and McMahon, T. A.** (1991). Mechanics of running under simulated low gravity.
311 *J. Appl. Physiol.* **71**, 863–870.
- 312 **Hedrick, T. L.** (2008). Software techniques for two- and three-dimensional kinematic measurements of
313 biological and biomimetic systems. *Bioinspir. Biomim.* **3**, 034001.
- 314 **Kram, R. and Taylor, C. R.** (1990). Energetics of running: A new perspective. *Nature* **346**, 265–267.
- 315 **Kuo, A. D.** (2001). A simple model of Bipedal Walking Predicts the Preferred Speed–Step Length Rela-
316 tionship. *J. Biomech. Eng.* **123**, 264.
- 317 **Long, L. L. and Srinivasan, M.** (2013). Walking, running, and resting under time, distance, and average
318 speed constraints: Optimality of walk–run–rest mixtures. *J. R. Soc. Interface* **10**, 20120980.
- 319 **McMahon, T. A. and Cheng, G. C.** (1990). The mechanics of running: How does stiffness couple with
320 speed? *J. Biomech.* **23**, 65–78.
- 321 **Rashevsky, N.** (1948). On the locomotion of mammals. *Bull. Math. Biophys.* **10**, 11–23.
- 322 **Ruina, A., Bertram, J. E. A. and Srinivasan, M.** (2005). A collisional model of the energetic cost of
323 support work qualitatively explains leg sequencing in walking and galloping, pseudo-elastic leg behavior
324 in running and the walk-to-run transition. *J. Theor. Biol.* **237**, 170–192.
- 325 **Selinger, J. C., O’Connor, S. M., Wong, J. D. and Donelan, J. M.** (2015). Humans can continuously
326 optimize energetic cost during walking. *Curr. Biol.* **25**, 2452–2456.
- 327 **Slawinski, J., Billat, V., Koralsztein, J.-P. and Tavernier, M.** (2004). Use of lumbar point for the
328 estimation of potential and kinetic mechanical power in running. *J. Appl. Biomech.* **20**, 324–331.
- 329 **Srinivasan, M. and Ruina, A.** (2006). Computer optimization of a minimal biped model discovers walking
330 and running. *Nature* **439**, 72–75.
- 331 **Willems, P. A., Cavagna, G. A. and Heglund, N. C.** (1995). External, internal and total work in
332 human locomotion. *J. Exp. Biol.* **198**, 379–393.
- 333 **Winter, D. A.** (2009). 4 Anthropometry. In *Biomechanics and Motor Control of Human Movement*, pp.
334 82–106. Hoboken, NJ: John Wiley & Sons, 4 edition.

335 **Figure legends**



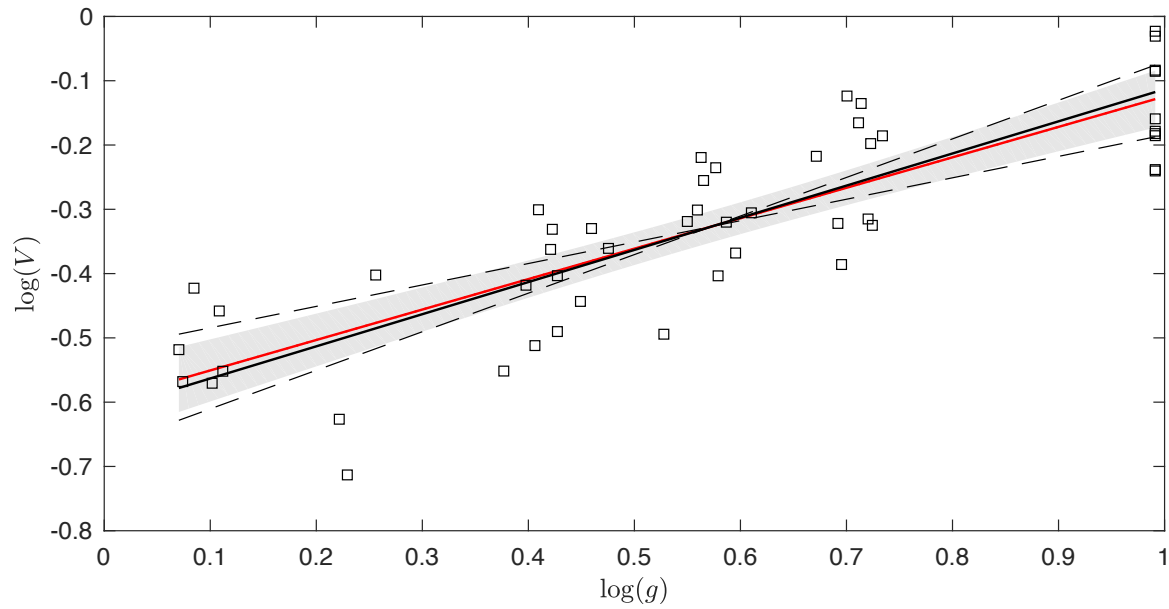
336

337 **Figure 1: Schematics explaining the energetic model.** (A) In the impulsive model of running, a point
 338 mass bounces off vertical, massless legs during an infinitesimal stance phase. As the horizontal velocity U
 339 is conserved, the vertical takeoff velocity V dictates the step frequency and stride length. Smaller takeoff
 340 velocities (light grey) result in more frequent steps that incur an energetic penalty, while larger takeoff
 341 velocities (dark grey) reduce the frequency penalty but increase losses during stance. The small box represents
 342 a short time around stance that is expanded in panel B. (B) We assume that the center-of-mass speed at
 343 landing is equal to the takeoff speed. The vertical velocity V and its associated kinetic energy are lost during
 344 an impulsive foot-ground collision of infinitesimally short duration. The lost energy must be resupplied
 345 through muscular work. Horizontal acceleration is assumed small and is neglected in the model.



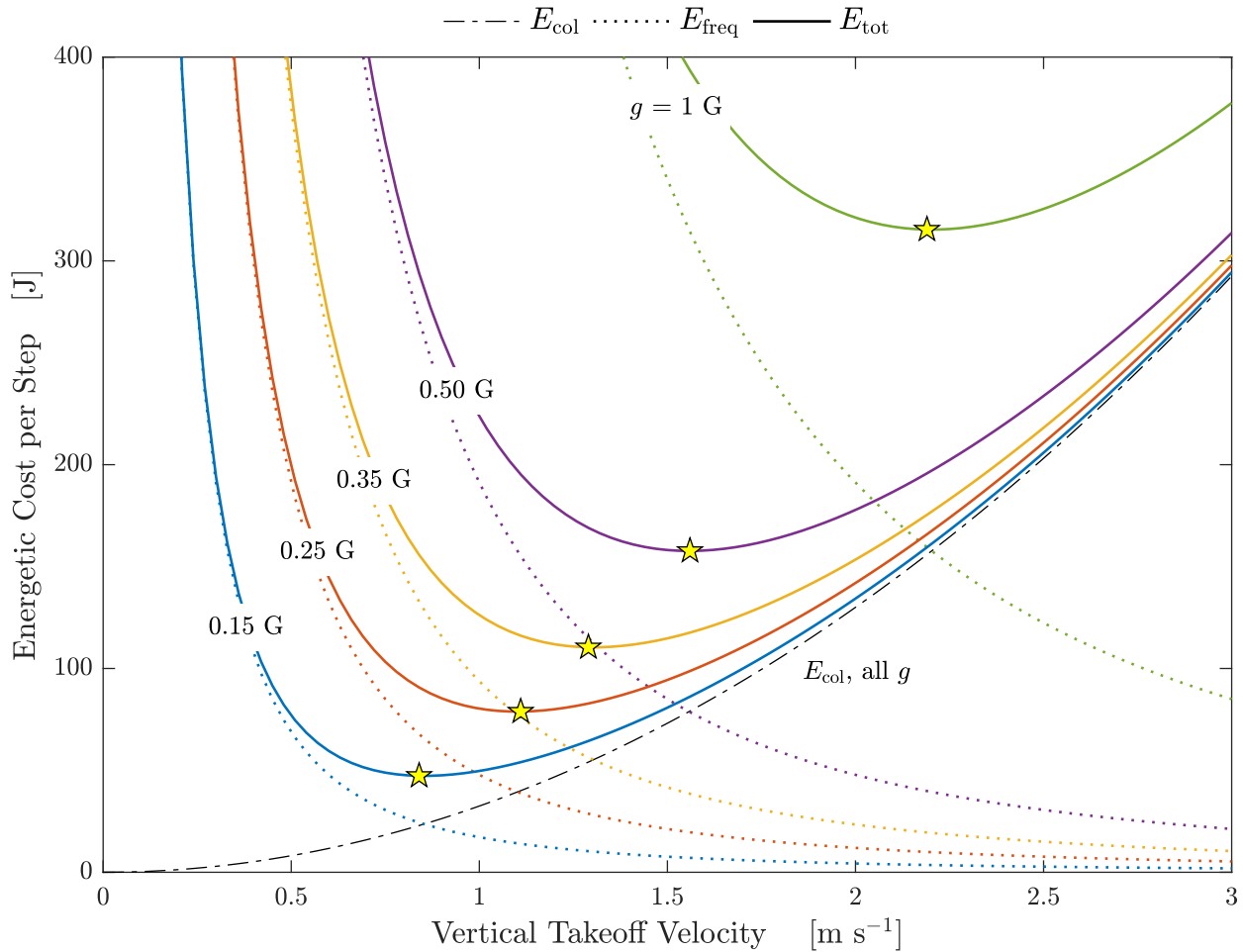
346

347 **Figure 2: Human subjects lower both ballistic height and takeoff velocity during running in**
348 **reduced gravity.** (A) Mean ballistic height (data points) increases with gravity (p of linear vs constant
349 model under two-tailed F -test: 4×10^{-4} , $N = 50$). The dashed line is the prediction for ballistic height
350 from the impulsive model, which deviates from observation at high g . The dash-dot line adds a correction
351 factor for finite stance time from the spring mass model (Eqn 3). This second prediction lies within the
352 95% CI of the least-squares linear fit (grey area). Both predictions use takeoff velocities from the best fit in
353 panel B. (B) Measured vertical takeoff velocities increase proportionally with the square root of gravitational
354 acceleration, following work-based energetic optimality. The least squares fit of the impulsive model with
355 $k = 2$ is shown as a dashed line. The fit has an R^2 value of 0.73 ($N = 50$). Each data point is a mean value
356 measured in one subject (ten subjects total) across multiple steps ($n \geq 50$) during a one-minute period at a
357 given gravity level. For both panels, if error bars (twice the s.e.m.) are smaller than the markers, then they
358 are not shown. Data used for creating these graphics are given in Table S1.



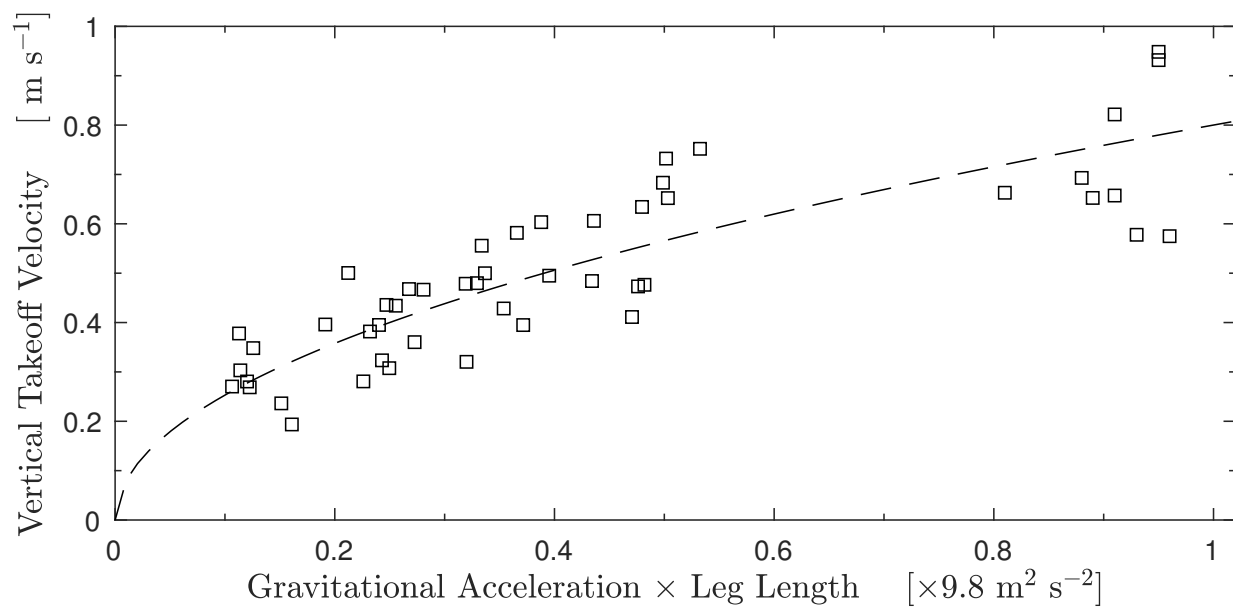
359

360 **Figure 3: A log-log plot of vertical takeoff velocity against gravitational acceleration shows that**
361 **the impulsive model yields the best fit when $E_{\text{freq}} \propto f^2$.** The least squares linear fit is shown in red
362 as a solid line, with 95% confidence interval as a grey area. The linear fit exhibits $R^2 = 0.70$ and a slope of
363 0.47 ± 0.09 (best estimate \pm 95% CI, $N = 50$), which is not significantly different from the predicted slope of
364 0.5 for $k = 2$ (black solid line), where k is the exponent relating frequency to cost ($E_{\text{freq}} \propto f^k$). Both $k = 1$
365 and $k = 3$ (shallow and steep dashed lines, respectively) yield predicted slopes (0.33 and 0.60 , respectively)
366 that lie outside the 95% CI, indicating that a work-based swing cost at $k = 2$ is a superior fit to the data,
367 while a simple linear frequency cost ($k = 1$) and an approximate force/time cost ($k = 3$, see Kuo 2001) do
368 not represent these data well. Data points are from ten subjects running at five gravity conditions each, and
369 each point is the mean of at least 64 takeoffs measured during each trial.



370

371 **Figure 4: The energetic costs according to the model are plotted as a function of vertical takeoff**
 372 **velocity (V) for the five levels of gravity tested.** The hypothetical subject has a mass of 65 kg and
 373 a frequency-based proportionality constant (A in $E_{\text{freq}} = Af^2$) derived from the best fit in Fig. 2B. Labels
 374 of gravity levels (g) are placed over the colours they represent. The collisional cost curve ($E_{\text{col}} = mV^2/2$,
 375 black dot-dash line) does not change with gravity, while the frequency-based energetic cost curve (E_{freq} ,
 376 dotted lines) is sensitive to gravity, leading to an effect on total energy per step (E_{tot} , solid lines). In lower
 377 gravity, a runner can stay in the air longer for a given takeoff velocity, so the associated frequency-based cost
 378 goes down. However, the cost of collisions at that same velocity is unchanged, since it depends only on the
 379 velocity itself. The relaxation of frequency-based cost allows the runner settle on a lower, optimal takeoff
 380 velocity (yellow stars) with both a lower frequency-based and collisional cost, compared to higher gravity.



381

382 **Figure A1: Vertical takeoff velocity scales with the square root of gravitational acceleration**
383 **times leg length during running.** The least squares fit for the model given by Eqn A4 is shown as a
384 dashed line. The fit exhibits $R^2 = 0.745$, using all fifty data points. Error bars (twice standard error of the
385 mean takeoff velocity measured during a trial, $n \geq 64$) are smaller than the marker size.

386 Appendices

387 A Cost of swing work in partial reduced gravity

388 The experimental apparatus (Hasaneini et al., 2017, preprint) unloads a subject's center of mass, but does
389 not act directly on their limbs. Consequently, while their center of mass might experience reduced weight,
390 the limbs swing under the influence of normal gravity. It is prudent to check how this affects the predictions
391 of the impulsive model.

The work required to swing a limb is (Doke et al., 2005)

$$E_{\text{swing}} \propto I(f^2 - f_n^2), \quad (\text{A1})$$

392 where I is the moment of inertia of the limb about the hip, f is the frequency of oscillation and f_n is the
393 natural frequency (equal to $\sqrt{g/l}$ for a simple pendulum, where l is leg length). Here we are assuming that
394 the limb changes configuration little during the swing phase, and so I is approximately constant. Note that
395 Eqn A1 is only valid when $f > f_n$ (Doke et al., 2005), since if sufficient time is available the limb can swing
396 passively. The swing frequency is slightly greater than the stride frequency⁴, which in the present study
397 ranged from trial-mean values of 0.69 to 1.47 Hz over all subjects and conditions (Table S1). Doke et al.
398 (2005) found the natural frequency of swinging legs to be 0.64 ± 0.02 Hz (mean \pm s.d.) for a subject group
399 with mean leg length of 0.88 ± 0.07 m (mean \pm s.d., $N = 12$). Our subject group exhibited larger mean
400 leg length (0.92 ± 0.06 m, mean \pm s.d., $N = 10$), so would very likely have smaller natural frequencies.
401 Therefore, the assumption that $f > f_n$ very likely holds in this case.

402 The leg moment of inertia about the hip scales approximately as $I \propto ml^2$, where m is body mass and l
is the leg length (Winter, 2009). Assuming $f = g/(2V)$, and invoking $E_{\text{tot}} = E_{\text{col}} + E_{\text{swing}}$, we have

$$E_{\text{tot}} = mV^2/2 + Bml^2 \left(\left(\frac{g}{2V} \right)^2 - f_n^2 \right), \quad (\text{A2})$$

404 where B is some proportionality constant. To achieve the energetically optimal takeoff velocity, we take the
derivative of Eqn A2 with respect to V , yielding

$$\frac{\partial E_{\text{tot}}}{\partial V} \Big|^{V=V^*} = mV^* - Bml^2 \frac{g^2}{2(V^*)^3} = 0, \quad (\text{A3})$$

406 where we note that any dependence on f_n has disappeared. However, there is a new dependence on l . Solving
Eqn A3 for V^* , we find

$$V^* \propto \sqrt{gl}. \quad (\text{A4})$$

408 Empirical V is plotted against gl in Fig. A1 with the least square fit of Eqn A4. The fit exhibits $R^2 =$
409 0.745, only a slight improvement compared to the simple impulsive model ($R^2 = 0.73$). Eqn A4 depends on
410 l , but if the variation in l is small, then Eqn A4 is indistinguishable from the simple swing-cost model (Eqn
411 2 with $k = 2$). Indeed, the leg lengths of our subject group varied only by a factor of 1.3 (range 0.81 to 1.04
412 m), while the highest experimental g was six times the smallest value. Since the variation in leg length was
413 comparatively small, it has little impact on the results.

⁴ Swing period is two flight phases and one stance phase, or one stance phase shorter than stride period.

414 B Ballistic height corrections from the spring-mass model

415 We seek to predict the vertical center-of-mass displacement achieved between takeoff (maximum vertical
416 velocity) and the maximum height during the flight phase. We know the maximum height from ballistics to
417 be $v^2/(2g)$, where v is the vertical velocity at toe-off. However, we do not know the displacement between
418 takeoff and toe off, nor do we know how to relate the velocity at takeoff to the velocity at toe-off. Both of
419 these unknowns could be calculated using the ground reaction force during stance, but this was not measured
420 empirically.

421 Instead, we can rely on the spring-mass model, which gives a decent approximation of the ground reaction
422 forces assuming the velocity at toe-off and natural angular frequency (ω_0) are given (McMahon and Cheng,
423 1990). In our case, the toe-off velocity is unknown, but the spring-mass model allows us to relate it to the
424 maximum vertical velocity, which can in turn be predicted by the impulsive model. ω_0 is defined as $\sqrt{k/m}$,
425 where k is the “spring” stiffness and m is mass. k is not actually the tendon stiffness, but is the virtual
426 stiffness generated by the motor control system during stance (Farley and Ferris, 1998; Donelan and Kram,
427 2000); that is, the muscle and tendon forces combine to generate ground reaction forces as if there were
428 one linear spring acting on the center of mass. The complicated interplay between muscles, tendons and
429 energetics makes the angular frequency hard to predict.

430 Fortunately, the vertical spring stiffness is held more-or-less constant through changes in gravity (He
431 et al., 1991), so we can use the empirically derived value⁵ of $\omega_0 \sim 18 \text{ rad s}^{-1}$. It remains simply to find the
432 displacement between takeoff and toe-off, and the vertical toe-off velocity, in terms of the vertical takeoff
433 velocity and gravity.

434 We follow McMahon and Cheng (1990) in assuming a point-mass body of mass m and massless legs.
435 We assume that the ground reaction force is well-approximated by the compression of a spring with angular
436 frequency ω_0 . For simplicity, we use a hopping model, which assumes that a person exhibits a small excursion
angle (*i.e.* $\theta \sim 0$). The leg length minus resting length is r , and so the dynamics of the system are

$$437 \quad \ddot{r} + \omega_0^2 r + g = 0, \quad (\text{B1})$$

438 where g is gravitational acceleration. Setting the vertical landing velocity to $\dot{r}(0) = -v$, and the initial
position as $r(0) = 0$, the solution to the ordinary differential equation is (McMahon and Cheng, 1990)

$$439 \quad \omega_0^2 r(t) = -\omega_0 v \sin(\omega_0 t) + g \cos(\omega_0 t) - g. \quad (\text{B2})$$

The instantaneous velocity is thus

$$440 \quad \dot{r} = -v \cos(\omega_0 t) - \frac{g}{\omega_0} \sin(\omega_0 t). \quad (\text{B3})$$

441 Eqns B1-B3 are valid for $0 \leq t \leq t_s$, where $t_s = (2\pi - 2 \arctan(\text{Gr}))/\omega_0$ is the stance period, and
442 we have introduced the non-dimensional Groucho number $\text{Gr} \equiv v\omega_0/g$ (McMahon and Cheng, 1990). For
443 $t_s < t < t_s + 2v/g$, the body is in a ballistic phase.

444 We can now determine the timing and magnitude of the peak vertical velocity. Let t^* correspond to any
445 time at which a maximum speed is achieved. Since Eqn B3 is continuous and periodic, local maxima and

⁵ This value was calculated by taking the average value of vertical stiffness data in Fig. 7 of He et al. (1991), dividing by average mass of subjects in the same study and taking the square root. 18 rad s^{-1} falls within all the error bars of Fig. 7, so seems representative of the natural angular frequency at all levels of gravity.

minima in velocity must satisfy $\ddot{r} = 0$. Therefore, from Eqn B1,

$$r(t^*) = -\frac{g}{\omega_0^2}. \quad (B4)$$

Combining Eqn B4 with B2 and solving for $0 \leq t^* \leq t_s$ yields

$$t^* = (\arctan(\text{Gr}^{-1}) + n\pi) / \omega_0, \quad n = 0, 1$$

corresponding to the points of maximal speed during stance. The second point ($n = 1$), corresponds to the time at which maximal velocity is achieved,

$$t_m = (\arctan(\text{Gr}^{-1}) + \pi) / \omega_0. \quad (B5)$$

To determine the peak velocity V , we insert Eqn B5 into B3. Using the relations $\cos(\arctan(x)) = 1/\sqrt{x^2 + 1}$ and $\sin(\arctan(x)) = x/\sqrt{x^2 + 1}$, we find

$$V = \frac{g}{\omega_0} \sqrt{\text{Gr}^2 + 1}, \quad \text{and}$$

$$v^2 = V^2 - (g/\omega_0)^2 \quad (B6)$$

In the main manuscript, we define the ballistic height (H) as the vertical displacement from the time of maximal vertical velocity to the maximum height achieved during a stride, that is,

$$H = \frac{v^2}{2g} - r(t_m). \quad (B7)$$

We need only insert Eqns B4 and B6 into Eqn B7 to find

$$H = \frac{V^2}{2g} + \frac{g}{2\omega_0^2}.$$

Note that the first term is identical to the prediction of the impulsive model (*i.e.* $V = v$), while the second term gives a correction from the spring mass model, due to finite stance time. Since we have established that $V = A\sqrt{g}$, the prediction for H in terms of g alone is

$$H(g) = \frac{A^2}{2} + \frac{g}{2\omega_0^2}. \quad (B8)$$